The vibrational spectrum of crystalline benzoic acid: Inelastic neutron scattering and density functional theory calculations

ARTICLE *in* THE JOURNAL OF CHEMICAL PHYSICS · AUGUST 2001

Impact Factor: 2.95 · DOI: 10.1063/1.1386910 · Source: OAI

5 AUTHORS, INCLUDING:

Marie Plazanet
University Joseph Fourier - Grenoble 1
61 PUBLICATIONS **724** CITATIONS
SEE PROFILE

Hans Peter Trommsdorff
University Joseph Fourier - Grenoble 1
60 PUBLICATIONS **865** CITATIONS
SEE PROFILE

The vibrational spectrum of crystalline benzoic acid: Inelastic neutron scattering and density functional theory calculations

M. Plazanet[a)]
Laboratoire de Spectrométrie Physique, Université Joseph Fourier de Grenoble-CNRS (UMR 5588), BP 87, 38402 St. Martin d'Hères Cx, France and Institut Laue-Langevin, BP 156, 38042 Grenoble Cx 9, France

N. Fukushima[b)] and M. R. Johnson
Institut Laue-Langevin, BP 156, 38042 Grenoble Cx 9, France

A. J. Horsewill
School of Physics & Astronomy, University of Nottingham, Nottingham, NG7 2RD, United Kingdom

H. P. Trommsdorff[c)]
Laboratoire de Spectrométrie Physique, Université Joseph Fourier de Grenoble-CNRS (UMR 5588), BP 87, 38402 St. Martin d'Hères Cx, France

(Received 21 February 2001; accepted 30 May 2001)

Vibrational spectra of several isotopomers of benzoic acid (BA) crystals have been recorded by inelastic neutron scattering and are compared with spectra calculated for different potential energy surfaces (PES). These PES were obtained within the harmonic approximation from quantum chemical density functional theory (DFT) calculations made for the monomer, the isolated dimer, and the crystal using different codes and different levels of basis functions. Without refinement of the force constants, agreement between calculated and observed spectra is already sufficient for an unambiguous assignment of all vibrational modes. The best agreement was obtained with periodic DFT calculations. The most prominent discrepancy between calculated and observed frequencies was found for the out-of-plane O–H bending modes. For these modes (as well as for the in-plane bending and the O–H stretching modes) the anharmonicity of the potential was calculated, and the anharmonic correction was shown to account for about one-third of the discrepancy. The origin of this difference is attributed to the slight compression of the hydrogen bonds in the calculated structure of the dimer, which also leads to a significant lowering of the frequency of the O–H stretch mode. © *2001 American Institute of Physics.* [DOI: 10.1063/1.1386910]

I. INTRODUCTION

The rapid development of computer power, together with the availability of efficient codes, has made the determination, by *ab initio* quantum chemical calculations, of potential energy surfaces (PES) increasingly reliable. This is true even for PES governing the motions of molecular systems of moderate size comprising hundreds of atoms. In order to assess the validity and limitations of such calculations, it is necessary to confront predictions derived from computed PES with experimental data. While equilibrium positions of the PES can be compared with structural data, the shape of the PES close to these positions is reflected in the vibrational spectrum. Vibrational frequencies, related to the curvature of the PES, are directly observed in the spectra, while the corresponding eigenvectors determine the line intensities. In IR and Raman spectroscopy the calculation of these intensities is subject to some uncertainty, requiring the knowledge of the derivatives along the normal modes of dipole moments and of polarizability tensors. In contrast, in vibrational spectra obtained by inelastic neutron scattering (INS), the scattering intensity is simply given by the product of the amplitude of the motion with the known scattering cross section of a nucleus, summed over all atoms of the system, so that precise predictions of INS spectra can be made for any given PES.[1,2] Of particular interest in the context of the present work is the fact that the scattering cross sections of the proton and the deuteron differ by a factor of 20, so that isotopic replacements, which at the level of the computations have no influence on the force field, lead to significant changes of the observed intensities. Selective deuteration can thus be employed to highlight the motion of a specific hydrogen atom.

While the shape of a PES near stable positions can be derived either from experimental data or from calculations, trajectories relating different stable configurations and saddle points between them can only be obtained via computations. This knowledge of transition states and reaction paths is essential for the understanding of the chemical dynamics of a system, so that the reliability of computational approaches becomes a central issue. With this motivation, the present work was undertaken in order to establish the ground state PES of the benzoic acid (BA) crystal as a benchmark model

[a)]Present address: University of Toronto, Department of Physics and Chemistry; 80, St Georg Street, Toronto, ON M5S 3H6, Canada.
[b)]Visiting scientist. Permanent address: SGI Japan Ltd., Yebisu Garden Place Tower, 4-20-3 Ebisu Shibuya-ku, Tokyo, 150-6031 Japan.
[c)]Author to whom correspondence should be addressed. Electronic mail: trommsdo@spectro.ujf-grenoble.fr

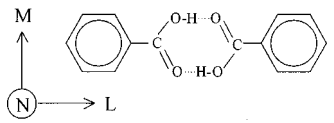

FIG. 1. Structure of benzoic acid dimers with indication of L, M, N axes.

system for proton transfer along hydrogen bonds and to thereby assess the reliability of available computational methods for calculating this PES.

BA, as many other carboxylic acids, forms symmetric dimers in the crystal, linked by two hydrogen bonds (Fig. 1). There exist two tautomers, which interconvert by a concerted transfer of the two acid protons. The hydrogen bond length and strength in these dimers, as well as the structural changes during the proton transfer, are typical for a large number of hydrogen bonded systems. In addition to the large amplitude motion of the protons, this reaction also involves a significant rearrangement of all other atoms, both of the molecular skeleton and of the environment. The PES, near the equilibrium positions, is well represented within the harmonic approximation and normal modes describe the dynamics. For the description of the proton transfer reaction, however, this separation of variables becomes invalid since none of the normal mode coordinates of the ground state points in the direction of the straight-line path connecting the equilibrium configurations of the two tautomers. In addition, force constants of all coordinates change along the reaction path. The PES describing the proton transfer is therefore multidimensional and cannot be reduced to a one-dimensional cut along the reaction coordinate. Much current effort is directed toward a proper description of this PES and a quantitative evaluation of the dynamics in this multidimensional PES.[3]

The choice of BA as a model system was motivated by several considerations: In isolated BA the two minima of the PES which correspond to the two tautomers are equivalent. While this symmetry is broken in the condensed phase, the resulting energy difference, *A*, between the two tautomers of BA is the smallest known of all crystals of carboxylic acid dimers. In the case of the BA crystal, it has been possible to reduce this energy difference in the vicinity of impurity guest molecules, doped intentionally into the crystal, to a level where the protons become sufficiently delocalized over the two wells of the PES that coherent tunneling could be observed, and the value of the tunneling matrix element, Δ,[4] was determined.[5] In addition, the proton correlation time in the pure crystal, τ_c, essentially determined by incoherent tunneling, was measured as a function of temperature and pressure by quasi-elastic neutron scattering and proton NMR T_1 measurements.[6–8] Of particular interest with respect to the present work was the identification of an activation energy of about 100 cm^{-1} in the temperature dependence of τ_c, which is attributed to thermally activated tunneling in the excited state of a vibration, which is coupled to the tunneling mode.

In this paper we present vibrational spectra of several isotopomers of BA obtained by inelastic neutron scattering, which are compared with spectra calculated for different PES. These PES were obtained within the harmonic approximation from quantum chemical (DFT) calculations made for the monomer, the isolated dimer and the crystal using different codes and different levels of basis functions. Even without having recourse to a refinement of the force constants, agreement between calculated and observed spectra is sufficient for an unambiguous assignment of all vibrational modes. The most prominent discrepancy between calculated and observed frequencies was found for the out-of-plane O–H bending mode. For this mode, as well as the in-plane O–H bending and stretching modes, the anharmonicity was calculated.

II. EXPERIMENTAL AND COMPUTATIONAL TECHNIQUES

A. Materials

Materials were as follows: fully protonated, C_6H_5COOH ($BA-H_6$), and ring deuterated, C_6D_5COOH ($BA-D_5H$), BA were commercial products, fully deuterated, C_6D_5COOD ($BA-D_6$), BA was obtained from $BA-D_5H$ by multiple exchange with heavy water; ^{18}O labeled, $C_6H_5C^{18}O^{18}OH$ ($BA-^{18}O$) BA was synthesized from correspondingly labeled water and subsequently exchanged with light water since the starting ^{18}O water was deuterated to about 80%. The isotopic purity of the deuterated compounds was determined to be $\geqslant$99% and that of the ^{18}O compound $\geqslant$98%. Prior to use, all materials were purified by extensive zone refining.

B. Spectra

Inelastic neutron scattering spectra were recorded on powdered samples at 20 K with the TFXA (now TOSCA) spectrometer at ISIS (Rutherford Appleton Laboratories).[9]

C. Computations

The harmonic force fields for the isolated molecule and the dimer were calculated, after geometry optimization, using the molecular orbital methods as implemented in GAUSSIAN98.[10] Different basis functions were investigated [6-311 G(d,p), 6-311+G(2d,p), and 6-311++G(3df,pd)] and electron exchange and correlation effects were determined using the B3LYP functional. In these approximations, force constants are obtained in analytical form, from which the force constant matrix is constructed.

The dimer calculation was repeated and a full crystal calculation was performed using the *ab initio* total-energy and molecular dynamics program VASP (Vienna *ab initio* simulation program).[11–13] All DFT calculations were performed using the recommended energy cutoff for the plane wave basis set (396 eV) with ultrasoft Vanderbilt pseudopotentials. For those aspects of the calculations performed in reciprocal space, a maximum *k*-point spacing of 0.01 $Å^{-1}$ was used. Exchange-correlation effects were handled within the generalized gradient approximation (GGA-Perdew Wang 91).

Since DFT-GGA underestimates dispersive interactions, geometry optimization of the periodic structures was limited to optimizing the atomic coordinates in the measured unit

TABLE I. Calculated and experimental bond lengths (Å) characterizing the hydrogen of benzoic acid dimers. (a) free dimer B3LYP; (b) VASP; (c) single crystal neutron diffraction, Ref. 19.

Bond	Free (a)	Crystal (b)	Exp. 20 K (c)
O·····O	2.715	2.561	2.608
O–H	1.022	1.037	0.995
H–H′	0.67	0.487	0.70

cell. While this approximation may effect the calculation of lattice modes, previous work with periodic DFT methods has shown that low frequency molecular vibrations are mainly sensitive to shorter-range (<10 Å) intermolecular interactions.[14–16]

With VASP, first derivatives in the form of Hellmann–Feynmann forces are available for all atoms in the cell. The force constant matrix was therefore constructed from single point energy (SPE) calculations on the 360 structures generated from the optimized structure by displacing each of the 60 atoms in positive and negative senses along the Cartesian directions *x, y, z* by 0.05 Å. A displacement of this size typically increases the energy of the unit cell by 0.05 eV (δ), ensuring that the induced forces are generally significantly greater than the numerical noise, while remaining in the regime of linear restoring forces. Each pair of SPE calculations (positive and negative displacements) enables a row of the force constant matrix, corresponding to a Cartesian displacement of one atom, to be determined, each force constant being a central difference $[(F_+ - F_-)/2\delta]$. Space group symmetry was not used to relate the force constants within the matrix. Convergence of the calculation of force constants was tested as a function of the energy cutoff, the *k*-point spacing, and the displacement size δ. No significant improvement could be obtained using values different to those quoted above.

From force constant matrices generated by GAUSSIAN and VASP, vibrational frequencies and eigenvectors were calculated for different isotopomers by diagonalizing the dynamical matrix constructed with the corresponding mass matrix. Inelastic neutron scattering spectra, including overtones, combinations (including combinations with lattice modes), were calculated from the normal modes using CLIMAX.[17,18]

III. RESULTS AND DISCUSSION

A. Background

Benzoic acid crystallizes in the form of centrosymmetric dimers (Fig. 1). The space group is $P2_1/c$ with two dimers, related by a 2_1 axis, per unit cell.[19] The monomer is very nearly planar and the mean planes, defined by the two monomers of a dimer, are separated by about 0.2 Å. This geometry was used as input of the geometry optimization of the calculations. Table I compares the experimental with the optimized geometries of the hydrogen bond in the BA dimer.

The 84 nonzero frequency modes of the isolated dimer are made up of 2×39 +/− combinations of the *intra*-monomer modes and 6 rotations and translations of the two monomer units relative to each other (*inter*-monomer modes). In the crystal, the factor group is C_{2h}, and the 177 nonzero frequency vibrations at wave vector $k=0$ can be described in the basis of 4×39 *intra*-monomer modes, 2×6 *inter*-monomer modes as well as 9 lattice modes comprising 6 rotations and 3 translations of the entire dimers.

The assignment of the vibrational modes of BA crystals has been the object of numerous prior studies, based on Raman and IR spectra as well as normal mode calculations.[20–28] Additional data on the ground state modes of free and matrix isolated BA dimers are available from IR and emission (fluorescence and phosphorescence) spectra.[29–32] The assignments of normal modes are sometimes partial and often controversial and it does not seem useful to discuss here the strengths and shortcomings of all these studies in detail. Overall and not unexpectedly, the general assignments of modes at higher frequencies are correct, even though the description of the eigenvectors may be imprecise or sometimes inverted between different observed frequencies. At lower frequencies, the assignments are hampered by the fact that, as discussed below, the lowest frequency *intra*- monomer mode lies in the range of *inter*-monomer and lattice modes. Because of these shortcomings, the existing force fields were found to be insufficient as a starting point for a refinement using the program CLIMAX and the observed neutron scattering spectra. No satisfactory simulation of these spectra was therefore obtained.[33] The same statement holds for normal mode calculations based on different generic force fields.[16] Because of the relatively large number of modes, this failure is not surprising.

In contrast, the force fields derived from DFT calculations reproduce, without any refinement of force constants, the measured spectra to an extent that the correspondence between calculated and observed modes are unambiguous for all frequencies above 150 cm^{-1}. Already in calculations for the isolated dimer this agreement is sufficient and is, interestingly, not significantly improved in increasing the basis set size beyond 6-G311G(d,p) with B3LYP. By making these calculations, both for the isolated monomer and dimer, the change of modes introduced by the hydrogen bonds and the resulting changes of force field and coupling of the two monomer units can be explored. This comparison is also useful for a description of the normal modes of the dimer in terms of those of the monomer. A shortcoming of these calculations is that they involve an overall scaling of the force field in order to reduce the calculated frequencies to the observed values.[34] In addition, the effect of intermolecular forces in the crystal is omitted in calculations on isolated molecules and dimers. Periodic DFT calculations, incorporating a plane wave basis set (VASP), were therefore used to calculate the force field of the crystal. For comparison, the same code was employed to obtain spectra of a single dimer quasi-isolated in the simulation box. Spectra obtained from these VASP calculations for a crystal were overall the most accurate and are shown together with the experimental spectra in Fig. 2 for the isotopomers BA–H_6, BA–D_5H, and BA–D_6. The spectral shifts for the BA–^{18}O isotopomer are too small to show up at the scale of these spectra and are therefore shown enlarged in Fig. 3 for the most relevant section of the spectrum only.[35] The effect of the ^{18}O substitution is immediately apparent for the modes involving motions of

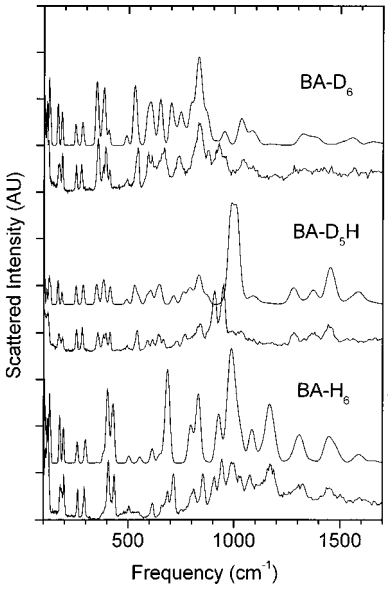

FIG. 2. Inelastic neutron scattering spectra of three isotopomers of Benzoic acid, BA–H_6, BA–D_5H, BA–D_6, together with the corresponding spectra calculated using the VASP code. Only the spectral region up to 1700 cm^{-1} is shown, at higher frequencies, because of the low resolution the spectra become uninformative.

the carbonyl group relative to the phenyl ring. As expected, for these modes the factor group *g u* splitting, indicated in the figure, is relatively large, representing essentially the coupling of the two monomers in a dimer. For the phenyl-carbonyl stretch mode, the second factor group *g* component lies at 414 cm^{-1} and is hidden by two intense out-of-plane ring deformation modes around 400 and 430 cm^{-1}.

B. Internal modes

The low frequency part (<120 cm^{-1}) of the spectrum, discussed later, is fairly well separated and comprises in addition to the external and *inter*-monomer modes the lowest frequency mode of the monomer, namely the torsion of the carbonyl group with respect to the benzene ring. All modes at higher frequencies are well described as more or less strongly coupled $+/-$ combinations of the monomer modes.

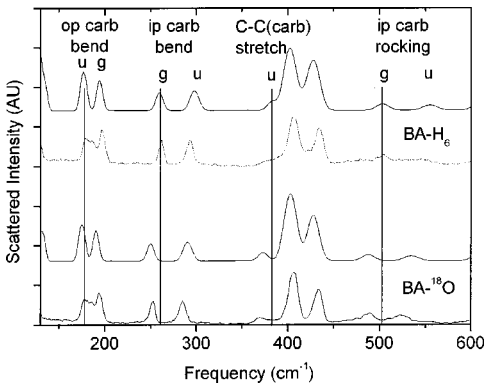

FIG. 3. Inelastic neutron scattering spectra of benzoic acid, BA–H_6 and BA–^{18}O. Upper curves: calculated using the VASP code; lower curves: experiment. Only the spectral region showing the most obvious isotope effects (modes of the carbonyl group) is represented.

In this part of the spectrum, agreement between the calculated and observed spectra is such that an unambiguous assignment of all modes is obtained. When different modes, being too close in frequency, are not separated in the experimental spectra, the comparison between the different isotopomers made it possible to lift any ambiguity. In order to avoid lengthy repetitions, the assignment is given in Table II for BA–D_5H only. The choice of this isotopomer is justified by the following: the participation of the acid hydrogen in the different modes is of particular interest, and by masking via H/D replacement the ring-proton motions, this participation is best visible for the BA–D_5H isotopomer. For the two other isotopomers BA–H_6 and BA–D_6, this participation is buried or not specifically visible. In addition, as it turned out, the description of modes is simpler for the BA–D_5H isotopomer.

Strictly, the 84 vibrations of the free dimer and the 177 vibrations of the crystal must be classified according to the respective symmetry groups, the center of inversion being the only symmetry element common to the two groups. All modes of the dimer can be described in terms of *g* and *u* combinations of modes of the monomer. Since the crystal field is only a small perturbation, most internal vibrations can in addition be well classified as being symmetric (in-plane, ip) or antisymmetric (out-of-plane, op) with respect to the molecular plane. For the free dimer, the ground state symmetry C_{2h} becomes D_{2h} in the transition state of the proton transfer reaction. As it turns out, many modes can in fact be approximately classified according to the D_{2h} group of the transition state geometry. This classification becomes inappropriate when modes close in frequency have the same symmetry species in C_{2h} or C_i. The classification is obviously inappropriate for modes involving the OH proton and the C–O and C=O stretch modes. For the BA–D_5H isotopomer, this approximate classification is given in Table II when appropriate. For the other isotopomers such a classification fails more frequently. The data in Table II, together with the spectra in Fig. 2, are self-explanatory and do not require detailed comments. As expected, for most vibrations the g/u splitting due to the coupling of the monomers within the dimer exceeds the $+/-$ factor group splitting, the exceptions involve modes of the benzyl ring. When resolved in the INS spectra, this g/u splitting agrees well with the calculated value.

It may be noted that the experimental spectrum exhibits a small rising background, which is absent in the calculated spectra. The issue of this background, commonly observed in INS spectra, has been discussed in Ref. 14 and is not relevant for the objectives of the present work. Regarding the vibrational modes, the only obvious and notable discrepancy between calculation and experiment involves the O–H op bending modes, for which the calculated mean value exceeds the experimental value by 7.3% (68 cm^{-1}) while the g/u splitting of 27 cm^{-1} is smaller than the observed value of 41 cm^{-1}. The incorrect location of this mode also perturbs neighboring modes, an effect particularly obvious in the BA–H_6 spectra. The ip O–H bending mode is mixed with ip C–C and C–O stretching modes, increasing the intensity of these modes without influencing too much their frequencies.

TABLE II. Comparison of calculated and observed internal frequencies of BA–D_5H [in cm^{-1}, colums (1), (2), (4), (5)]. Results of GAUSSIAN (B3LYP) for the isolated monomer and dimer together with the approximate symmetry in D_{2h} [columns (1)–(3)]. Results of VASP for the quasi-isolated dimer (4) and for the crystal (5), for which the frequencies of the two exciton components are given in the order of symmetry +/− with respect to the $C2_1$ axis of the crystal. For simplicity, exciton and g/u dimer splittings are not given when this splitting is smaller than about 1% of the frequency and thus unresolvable in the INS spectra. In this case only the center of gravity of the intensity is given. Intensity calculated with VASP (6). Frequencies observed in INS (7) and description of the mode (8). Note that for a better correlation between the different columns, the frequencies are not always in strictly increasing order.

(1) *G*-mon	(2) *G*-dim	(3) sym D_{2h}	(4) *V*-iso	(5) *V*-xtal	(6) Int.	(7) INS	(8) Mode
70	72	$b1g$	mixed with external				op carb twist
	90	au	modes (Table IV)				
149	158	$b3u$	139	165/169	2.7	172	op carb bend
	177	$b2g$	164	185/187	1.3	189	
209	256	$b3g$	258	253	2.5	256	ip carb bend
	276	$b2u$	289	288/284	3.3	283	
361	361	au	334	354/347	2.3	357	op ring twist
	361	$b1g$	352	353/346	2.2		
377	418	ag	417	414	3.6	414	ip carb stretch
	382	$b1u$	390	376	2.0	382	
393	401	$b3u$	374	383	2.4		op ring bend
	404	$b2g$	378	387	2.0	393	
485	501	$b3g$	489	491	1.2	494	ip carb rocking
	539	$b2u$	544	550/544	2.3	542	
546	549	$b3u$	506	531/524	2.6		op CD bend
	549	$b2g$	522	533/527	2.6		
607	607	$b3g/b2u$	585	587	2.5	591	ip ring def
630	624	$b3u$	603	608/601	2.1	614	op CD bend
	626	$b2g$	614	611/603	2.1		
644	653	ag	632	634	3.3	642	ip carb+ring angle bend
	659	$b1u$	641	647	1.6	650	
674	673	$au/b1g$	650	656	4.0	666	op CD bend
744	742	$b3u/b2g$	710	713	3.0	730	op CD bend
747	774	ag	755	758	3.9	760	ip CD+carb bend
	790	$b1u$	775	789	2.5	770	
811	811	$b1g/au$	787	791	2.7		op CD+ring bend
822	822	$b2g/b3u$	793	798	2.4		op ring+CD+carb bend
833	833	$b3g/b2u$	807	820	4.6		ip CD bend
846	849	$ag/b1u$	828	832	6.4	830	ip CD bend
867	864	$b2g/b3u$	832	834			op ring twist
859	859	$b3g$	836	839/849	2.2	841	ip CD bend
	859	$b2u$	841	840/847	2.1		
881	881	$b1u/ag$	864	870	3.7	873	ip CD bend
581	954	g	1018	983	40	908	op OH bend
	998	u	1053	1010	38	949	
975	975	$b1u/ag$	952	953	1.9		ip ring breath
1051	1055	$b3g/b2u$	1023	1029	2.9	991	ip CD bend
1083	1109	$b1u/ag$	1083	1088	1.4	1032	ip ring def+C-carb stretch
1185	1301	g	1272	1274	4.2	1282	ip OH bend+CC+CO stretch
	1310	u	1284	1285	5.1		
1336	1338	$b3g/b2u$	1351	1359	1.6		ip ring CC stretch
1364	1364	$b3g/b2u$	1325	1327	1.2		ip ring CC stretch
1344	1404	$b1u/ag$	1368	1374	7.4	1375	ip OH+bend+CC+CO stretch
1423	1475	u	1442	1447	14.9	1450	ip OH+ring bend+CC stretch
	1502	g	1462	1462	10.6		
1590	1589	$b2u/b3g$	1544	1550	1.5		ip CC stretch
1610	1610	$b1u/ag$	1564	1566	1.2		ip CC stretch

TABLE II. (*Continued.*)

(1) *G*-mon	(2) *G*-dim	(3) sym D_{2h}	(4) *V*-iso	(5) *V*-xtal	(6) Int.	(7) INS	(8) Mode
1802	1695	*g*	1592	1590	7.3		ip CC+CO stretch+OH
	1744	*u*	1650	1658/1641	1.1		bend
2335–2376	2335–2377		2288–2331	2299–2341	5.0		ip CD stretch
3772	3085	*g*	2574	2494/2499	8.5		ip OH stretch
	3188	*u*	2733	2667/2631	7.6		

Nevertheless, the calculated center of gravity of the intensity of these modes between 1250 and 1600 cm^{-1} lies at somewhat higher frequency as compared to the spectra, indicating that the force constant of this mode may also be overestimated. In contrast, the calculated frequencies of the O–H stretch modes at 2490/2630 cm^{-1}, which, as all higher frequency modes, is not observed in the INS spectra, are clearly lower than the generally accepted literature values as deduced from IR or Raman spectra. It is plausible that all these discrepancies are linked to the fact the hydrogen bond length of BA, calculated in VASP, is shorter than the experimental value (see Table I). This shortening of the hydrogen bond length is not an effect of compression by the crystal, since similar values were obtained in VASP calculations for the quasi-isolated dimer. It is known that the O–H modes are extremely sensitive to the geometry of the hydrogen bond, and the observed differences are consistent with a shorter hydrogen bond. Nevertheless, for these large-amplitude vibrations anharmonicity is also expected to be important with the result that the values calculated within the harmonic approximation are systematically higher than the values corresponding to the anharmonic potential. For the O–H modes we have therefore investigated this correction and have calculated the energy as a function of displacement for hydrogen atom displacements of up to 0.2 Å (stretch) and 20° (bend). The calculated potential curves are perfectly fitted by a quartic potential function:

$$V=\frac{\kappa}{2}x^2+\lambda x^3+\mu x^4. \tag{1}$$

The coefficients, κ, λ, μ, are given, in Table III. The anharmonic 0-1 transition energies have been evaluated by the second order perturbation expression:[36]

TABLE III. Coefficients of the quartic potential: $\frac{1}{2}\kappa X^2+\lambda X^3+\mu X^4$, describing the symmetric (*g*) and antisymmetric (*u*) O–H stretch (ν), ip bend (δ), and op bend (γ) modes. Energy is in units of eV, coordinates in units of Å or rad. The resulting anharmonic frequency correction is given in the last column.

Mode	κ	λ	μ	$\nu_a-\nu_h$ [cm^{-1}]
ν_gO–H	42.2	+93.2	+154.2	−430
ν_uO–H	49.4	+0.03	+153.7	+156
δ_gO–H	16.2	−1.91	−5.22	0
δ_uO–H	15.2	+0.01	−5.08	−16
γ_gO–H	8.1	−0.24	−3.26	−19
γ_uO–H	8.3	−0.003	−3.37	−19

$$E_1-E_0=\hbar\omega\left(1+\hbar\omega\left(\frac{3\mu}{\kappa^2}-\frac{15}{2}\frac{\lambda^2}{\kappa^3}\right)\right). \tag{2}$$

The resulting frequency corrections (i.e., the differences between the anharmonic and harmonic transition frequency, $\nu_a-\nu_h$,)) are also indicated in Table III. While the corrections are substantial for the O–H stretch modes, they explain only one-third of the difference observed for the O–H out-of-plane bending modes, so that the dominant cause is the incorrect calculated length of the hydrogen bond.

C. Low frequency modes

The low frequency part of the spectrum, <140 cm^{-1}, is not well resolved in the INS spectra. In contrast to IR and Raman, INS spectra are not limited by the $k=0$ selection rule so the large number of modes together with the significant *k*-vector dispersion make this low frequency spectral region quasi-continuous. The *k*-vector dispersion is not determined in the VASP calculation, restricted to a single unit cell. This calculation does, however, give the factor group splitting at $k=0$. For these reasons, we include here single crystal IR[26] and Raman[37] data, obtained at liquid helium temperatures, in the discussion. Regarding the intensity and spread of the spectrum, however, overall agreement between the VASP calculation and the INS spectra is still remarkably satisfactory.

In addition to the 6 external modes of each monomer unit (3 translations and 3 rotations), the carbonyl torsion lies in the same frequency range so that there is a total of $7\times4=28$ modes in the low frequency region. Of these, 3 correspond to overall translations and the remaining 25 nonzero frequency modes are listed in Table IV. These modes correspond to $7ag$, $7bg$, $6au$, and $5bu$ modes. In IR, all 11 *u* modes are observed but only 11 of the 14 Raman active *g* modes have been resolved. Other low frequency modes, included in Table II (carbonyl op and ip bending modes at 158 cm^{-1} and 217 cm^{-1}) are slightly mixed with these modes. The ^{18}O isotope effect clearly validates the assignment of the carbonyl torsion in the frequency range of 86–89 cm^{-1}. Similarly, the inter-monomer stretch can be assigned to the two highest frequency modes and the ip rocking mode of the monomers relative to each other to the next ag/bg pair. At lower frequencies, the calculations indicate a significant mixing of the other modes derived from translations and rotations of the monomer units. This is the reason why, in spite of a good overall agreement at higher frequencies, the iso-

TABLE IV. BA crystal IR and Raman data–low frequency region, compared with VASP calculation. The factor group symmetry is indicated. The frequencies for BA–H_6 are given in cm^{-1}, and the % change with respect to these values is given for the other isotopomers.

IR data[a]			Calculation (VASP)				Raman data[b]	
	BA–H_6	%–D_5H		BA–H_6	%–D_5H	%–^{18}O	BA–H_6	%BA–^{18}O
au	25.1	0.4	*au*	26.5	1.5	2.3		
bu	35.9	1.1	*au*	30.9	2.3	1.6		
au	41.2	1.7	*bu*	35.6	2.8	1.4		
bu	71.5	4.6	*au*	40.3	2.2	1.7		
			ag	48.9	2.7	0.6	34.0	0.9
			g	69.0	3.5	0.9	51.9	1.4
			bg	74.0	4.2	0.8	55.5	0.9
			ag	81.2	5.0	1.5	60.3	1.2
			ag	86.3	4.3	3.6	88.7	4.7
			ag	87.8	3.9	2.8	97.4	1.5
			bg	89.0	3.8	2.8	99.5	2.1
au	79.2	4.4	*au*	96.9	5.8	1.3		
au	94.5	4.1	*u*	97.1	4.7	1.2		
bu	101.1	4.0	*bu*	102.7	5.0	1.5		
au	108.6	4.7	*au*	105.0	5.1	1.3		
			g	107.3	3.8	1.8		
bu	110.8	4.1	*bu*	112.4	5.9	1.6		
			g	118.4	4.2	2.2		
			g	121.4	4.2	2.1	119.6	1.3
			bg	127.4	3.5	3.6		
			ag	127.6	1.9	1.1	125.0	1.8
au	125.9	3.4	*u*	129.0	2.2	5.8		
bu	127.2	3.7	*bu*	130.6	3.0	2.1		
			bg	133.4	2.6	1.3	126.7	
			ag	136.3	2.2	1.5	132.8	2.2

[a]Reference 28.
[b]Reference 36.

tope effects are not always well reproduced, since many of the modes are quite close in frequency and small changes of force constants lead to large changes of the mode mixing. At the lowest frequencies, the discrepancies are most significant. Clearly, without adjustment of force constants, the precision of the calculation is not sufficient to reproduce the spectra. In addition, the VASP calculation also reflects the imprecise separation of *intra*-dimer and *inter*-dimer forces. Some indication of the contribution of the different motions to the observed modes is obtained from the isotope effects, which for translations are −1.63% for BA–^{18}O, and −2.03% for BA–D_5H with respect to the normal BA–H_6.

For completeness, we indicate the six modes of the isolated dimer, corresponding to relative rotations (R)/translations (T) of the monomer moieties around/along the (L, M, N) axes. The frequencies (in cm^{-1}) of these modes have been calculated with GAUSSIAN B3LYP as follows: R_M 17.8, R_L 35.0, R_N 60.0, T_N 63.6, T_M 107, T_L 116.5.

IV. CONCLUSION

The excellent overall agreement between the calculated and measured vibrational spectra of the BA crystal demonstrates that for systems as large as this, with 60 atoms in the unit cell, reliable force fields can be obtained directly, without adjustment of force constants, from periodic DFT calculations. Comparison of the calculations for the isolated monomer and dimer, as well as the crystal, shows that the most important couplings are within one dimer, and that the coupling of dimers within the crystal is fairly small for most vibrational modes. This is expected for BA where the two monomers are linked by two hydrogen bonds, while the inter-dimer interactions are dominated by van der Waals forces. The only weakness of the calculation is the slightly incorrect representation of the hydrogen bond geometry, leading to errors in the modes involving predominantly O–H motions. To investigate the origin and possible remedies of this deficiency is beyond the scope of the present work. Indeed, it is because of the excellent agreement for all other modes that a complete vibrational assignment could be achieved here and this deficiency was detected.

Regarding the proton transfer reaction in the benzoic acid crystal, no complete theoretical analysis of the active vibrations, i.e., the vibrations coupled to the proton transfer coordinate, has yet been made. The present work shows that the level of calculations presented here should be adequate to arrive at a description of the transition state, which enables such a treatment. Based on an analogous theoretical treatment of the formic acid dimer,[38] the two vibrations for which the tunneling splitting increases significantly in the excited state are the inter-monomer stretch and rocking modes. The frequencies calculated for these modes (129–136 cm^{-1}) are in very good agreement with the activation energy derived from the temperature dependence of the proton correlation time (125 cm^{-1}).[6]

ACKNOWLEDGMENTS

The authors are very grateful to Herbert Zimmermann, who has synthesized the ^{18}O labeled compound and to the

former thesis students and postdoctoral fellows Lukas von Laue, Richard I. Jenkinson, and Dermot F. Brougham, who have participated at some early stages in this work. Stewart F. Parker and John Tomkinson provided help and useful discussions during the measurements at ISIS. The discussions with Don Kearley have always been stimulating and useful. The authors are grateful to the Center Grenoblois de Calcul Vectoriel of the Commissariat à l'Energie Atomique (CEA-Grenoble) for the use of computing resources.

[1] M. R. Johnson, G. J. Kearley, and J. Eckert, Eds., ''Condensed phase structure and dynamics: A combined neutron scattering and numerical modeling approach,'' Chem. Phys. **261**, 1 (2000).
[2] J. Eckert and G. J. Kearley, Eds., ''Spectroscopic applications of inelastic neutron scattering: Theory and practice,'' Spectrochim. Acta **48**, 269 (1992).
[3] V. A. Benderskii, E. V. Vetoshkin, I. S. Irgibaeva, and H. P. Trommsdorff, Chem. Phys. **262**, 392 (2000), and references therein.
[4] Δ is defined as the ground state level splitting in a symmetric PES with two equivalent minima.
[5] A. Oppenländer, Ch. Rambaud, H. P. Trommsdorff, and J. C. Vial, Phys. Rev. Lett. **63**, 1432 (1989).
[6] M. Neumann, D. F. Brougham, C. J. McGloin, M. R. Johnson, A. J. Horsewill, and H. P. Trommsdorff, J. Chem. Phys. **109**, 7300 (1998), and references therein.
[7] A. J. Horsewill, D. F. Brougham, R. I. Jenkinson, C. J. McGloin, H. P. Trommsdorff, and M. R. Johnson, Ber. Bunsenges. Phys. Chem. **102**, 317 (1998).
[8] M. A. Neumann, S. Craciun, A. Corval, M. R. Johnson, A. J. Horsewill, V. A. Benderskii, and H. P. Trommsdorff, Ber. Bunsenges. Phys. Chem. **102**, 325 (1998).
[9] http://www.nd.rl.ac.uk/molecularspectroscopy/tfxa/index.htm
[10] M. J. Frisch, G. W. Trucks, H. B. Schlegel *et al.*, GAUSSIAN98, Revision A.5, Gaussian Inc., Pittsburgh, PA, 1998.
[11] G. Kresse and J. Hafner, Phys. Rev. B **47**, 558 (1993); *ibid.* **49**, 14251 (1994).
[12] G. Kresse and J. Furthmüller, Comput. Math. Sci. **6**, 15 (1996).
[13] G. Kresse and J. Furthmüller, Phys. Rev. B **54**, 11169 (1996).
[14] M. Plazanet, M. R. Johnson, J. D. Gale, T. Yildirim, G. J. Kearley, M. T. Fernández-Díaz, D. Sánchez-Portal, E. Artacho, J. M. Soler, P. Ordejón, A. Garcia, and H. P. Trommsdorff, Chem. Phys. **261**, 189 (2000).
[15] G. J. Kearley, M. R. Johnson, M. Plazanet, and E. Suard, J. Chem. Phys. **115**, 2614 (2001).
[16] M. Plazanet, thesis, Université Joseph Fourier, Grenoble 2000.
[17] G. J. Kearley, J. Chem. Soc., Faraday Trans. **82**, 41 (1986).
[18] G. J. Kearley, Nucl. Instrum. Methods Phys. Res. A **354**, 53 (1995).
[19] C. C. Wilson, N. Shackland, and A. J. Florence, J. Chem. Soc., Faraday Trans. **92**, 5051 (1996).
[20] S. Hayashi and N. Kimura, Bull. Inst. Chem. Res., Kyoto Univ. **44**, 335 (1966).
[21] L. Colombo and K. Furic, Spectrochim. Acta **27**, 1773 (1971).
[22] S. Hayashi and J. Umemura, J. Chem. Phys. **60**, 2630 (1974).
[23] G. Klausberger, K. Furic, and L. Colombo, J. Raman Spectrosc. **6**, 277 (1977).
[24] Y. Kim and K. Machida, Spectrochim. Acta **42**, 881 (1986).
[25] K. Furic and J. R. During, Chem. Phys. Lett. **126**, 92 (1986).
[26] R. Nakamura, K. Machida, M. Oobatake, and S. Hayashi, Mol. Phys. **64**, 215 (1988).
[27] S. Hayashi, M. Oobatake, R. Nakamura, and K. Machida, J. Chem. Phys. **94**, 4446 (1991).
[28] H. R. Zelsmann and Z. Mielke, Chem. Phys. Lett. **186**, 501 (1991).
[29] K. Furic and L. Colombo, J. Raman Spectrosc. **17**, 23 (1986).
[30] I. D. Reva and S. G. Stepanian, J. Mol. Struct. **349**, 337 (1995).
[31] S. G. Stepanian, I. D. Reva, E. D. Radchenko, and G. G. Sheina, Vib. Spectrosc. **11**, 123 (1996).
[32] J. C. Baum and D. S. McClure, J. Am. Chem. Soc. **102**, 720 (1980).
[33] D. Brougham (unpublished).
[34] H. Yoshida, A. Ehara, and H. Matsuura, Chem. Phys. Lett. **325**, 477 (2000).
[35] See EPAPS Document No. E-JCPSA6-115-516131 for calculated eigenfrequencies, eigenvectors, and intensities of the vibrations of all isotopomers. This document may be retrieved via the EPAPS homepage (http://www.aip.org/pubservs/epaps.html) or from ftp.aip.org in the directory /epaps/. See the EPAPS homepage for more information.
[36] Y. Ayant and E. Belorizky, *Cours de Mécanique Quantique* (Dunod, Paris, 2000).
[37] L. von Laue, Thesis, Université Joseph Fourier, Grenoble 1997.
[38] V. A. Benderskii, E. V. Vetoshkin, L. von Laue, and H. P. Trommsdorff, NASA Conf. Publ. **219**, 143 (1997).